

Rheology of thin films from flow observations

B. Figliuzzi · D. Jeulin · A. Lemaître ·
G. Fricout · J. J. Piezanowski · P. Manneville

Received: 21 January 2012/Revised: 25 July 2012/Accepted: 28 July 2012/Published online: 19 August 2012
© Springer-Verlag 2012

Abstract A major challenge regarding thin films is the characterization of their rheology and the measurement of the fluid physical parameters. For complex fluids, performing direct rheology measurements is extremely difficult considering the geometric characteristics of thin films. In this paper, we present a method for characterizing the film rheology based on measurements at regular time intervals of the film surface topography. These measures allow us, by solving an inverse problem, to validate a model of rheology for the thin fluid film and to determine the physical parameters specific to this model.

1 Introduction

Many industrial processes involve the flow of thin films over rough surfaces. For instance, the surface levelling of such films is of particular interest in the paint industry, since levelling largely determines the final topography and consequently the visual appearance of the painted surface. The study presented here is part of a larger research

project, which aims at optimizing the roughness of the surfaces on which the paint is deposited to improve their visual quality at the end of the painting process. To this end, a first step is to be able to model the rheology of the paint with enough accuracy and to simulate numerically the levelling process. The technique presented in this article allows one to access the rheology parameters that govern the levelling of paint, which are very difficult to measure directly for a thin liquid film.

Thin films have received considerable attention in the literature. A first major contribution is that of Orchard (1961), who considered film levelling within the framework of the lubrication approximation, which permits a substantial simplification of the Navier–Stokes equations. In his model, Orchard only considered Newtonian fluids that do not evaporate. For such films, he showed that the levelling dynamics is the result of an interplay between surface tension, as capillary forces tend to smoothen the topography, and the fluid viscosity, which limits the flow induced by the levelling. Later, Overdiep (1986) investigated the case of evaporating Newtonian thin films. Considering a fluid made of a solvent and a resin, he showed that local surface tension variations strongly affect the dynamics of the thin film levelling. Surface tension is strongly dependent on the solvent concentration within the film. In thinner areas where solvent evaporates more quickly, its value can vary significantly. The resulting surface tension gradient creates a shearing effect at the film surface known as the Marangoni effect. It was shown by Evans et al. (2000) that this shearing effect can lead to the formation of crater patterns on the surface of the paint during drying. However, for the topographies studied here, numerical simulations of the levelling have been performed (Figliuzzi et al. 2012), which show that Marangoni effect can be neglected. The thickness variations of the film are

B. Figliuzzi (✉) · D. Jeulin
Centre de Morphologie Mathématique,
École des Mines ParisTech, 77300 Fontainebleau, France
e-mail: figliuzzi.bruno@gmail.com

A. Lemaître
UMR Navier, 2 allée Kepler, 77420 Champs-sur-Marne, France

G. Fricout · J. J. Piezanowski
ArcelorMittal Global R&D, 57283 Maizières-lès-Metz
Cedex, France

P. Manneville
Hydrodynamics Laboratory, UMR7646,
École Polytechnique, 91128 Palaiseau, France

indeed quite small in our case. Wilson (1993) and later Howison et al. (1997) contributed to improve Overdiep's model. The effect of the substrate topography was studied by Weidner et al. (1996) in the two-dimensional case, and Eres et al. (1999) and Schwartz et al. (2001) in the three-dimensional case. Gaskell et al. (2004, 2006) finally considered the generalization of the different models to the case of inclined substrates, where gravity plays a significant physical role in the flow dynamics. A generalization of the model to non-Newtonian fluids was also considered by O'Brien and Schwartz (2002).

The rheology of fluids used in industrial processes is often complex and largely determines the levelling dynamics of thin films. The composition of the paint also influences the dynamics, since spatial variations of the solvent concentration can induce a shearing effect on the surface. A major challenge regarding the study of thin films is consequently the characterization of the fluid rheology and the measurement of the physical parameters. For complex fluids, performing direct in situ rheology measurements is extremely difficult considering the geometric characteristics of thin films. The experimental validation of the models is therefore often based on topography data relative to the film surface during its evolution. In this paper, we present an in situ characterization of the film rheology based on measurements of the topography of the film surface at regular time intervals. By solving an inverse problem, these measures allow us first to validate a rheological model for the fluid constituting the thin film and next to determine its rheological parameters. This method was applied to the study of a lacquer used in the automotive industry. A wavefront sensor developed by Phasics™ enabled precise monitoring of the topography evolution during the painting process and allowed us to gather a large experimental database.

In Sect. 2, the mathematical model used to describe the evolution of the painted film topography is described, and a theoretical approach of the inverse problem is presented. The method is applied to characterize the rheology of a lacquer used in the automotive industry. Section 3 is devoted to the presentation of the experimental data obtained with the wavefront sensor for this paint. The application of the method is described and discussed in Sect. 4. Conclusions are drawn in Sect. 5.

2 Mathematical model

We consider the levelling of a thin incompressible fluid film deposited on an horizontal substrate. The topography of the substrate is denoted as $S_a(x, y)$, the film thickness as $e(x, y, t)$, and the height of the free surface of the film as $h(x, y, t)$. An order of magnitude of the roughness is

$S_a = 5 \mu\text{m}$. At the beginning of the levelling, the film thickness is approximately $H = 70 \mu\text{m}$. A typical value of the paint velocity is $U = 10 \mu\text{m/s}$. The Reynolds number $Re = \rho U H / \eta$ is then approximately $Re \cong 7.8 \times 10^{-7}$. The Ohnesorge number of the film flow, which relates the viscous forces to inertial and surface tension forces, is

$$Oh = \frac{\eta}{\rho \gamma L},$$

where L denotes a characteristic length in the horizontal direction. With $\eta = 0.9 \text{ Pa s}$, $\rho = 1,000 \text{ kg/m}^3$, $\gamma = 2.71 \times 10^{-2} \text{ N/m}$ and $L = 150 \mu\text{m}$, we find $Oh \cong 221$, which indicates a preponderant influence of the viscosity in the levelling phenomenon.

In what follows, the levelling process will be studied within the framework of the lubrication approximation. More elaborate theories can be developed from the Navier–Stokes equations (Oron et al. 1997; Ruyer-Quil and Manneville 1998, 2000). The lubrication approximation is based on two observations: firstly, as the thin film flow is very slow, it becomes possible to use the Stokes equation to study the film evolution; secondly, as the thickness of the film is much smaller than the wavelength of the modulations along the surface, the fluid velocity is essentially directed in the horizontal direction. These considerations allow a substantial simplification of the equations describing the flow of the film.

2.1 Direct flow calculation

The thin film flow is governed by the Stokes equation

$$-\nabla p + \nabla \cdot \bar{\sigma} = 0, \tag{1}$$

where $\bar{\sigma}$ denotes the deviator stress tensor and p the local pressure within the film. Letting u and v be the velocity components along x and y , the z -component of the velocity and the gradients of u and v along x and y being neglected within the lubrication approximation, the strain rate tensor reads:

$$\frac{1}{2} (\nabla \mathbf{u} + {}^T \nabla \mathbf{u}) = \begin{pmatrix} 0 & 0 & \frac{1}{2} \frac{\partial u}{\partial z} \\ 0 & 0 & \frac{1}{2} \frac{\partial v}{\partial z} \\ \frac{1}{2} \frac{\partial u}{\partial z} & \frac{1}{2} \frac{\partial v}{\partial z} & 0 \end{pmatrix}. \tag{2}$$

The deviator stress tensor can be expected to be parallel to the strain rate tensor. Tensor $\bar{\sigma}$ then reads

$$\bar{\sigma} = \begin{pmatrix} 0 & 0 & \sigma_{xz} \\ 0 & 0 & \sigma_{yz} \\ \sigma_{xz} & \sigma_{yz} & 0 \end{pmatrix}. \tag{3}$$

Boundary conditions are given by a no-slip kinematic condition at the substrate surface, $u(z = S_a) = 0$, $v(z = S_a) = 0$, and by a mechanical condition

expressing that the constraint is zero at the free surface, $\partial u/\partial z(z = h) = 0$, $\partial v/\partial z(z = h) = 0$. Consequently:

$$\begin{cases} \sigma_{xz} = -\frac{\partial p}{\partial x}(h - z), \\ \sigma_{yz} = -\frac{\partial p}{\partial y}(h - z). \end{cases} \quad (4)$$

The pressure is defined as the product of the surface tension γ and the free surface curvature C . Within the lubrication approximation, at lowest order,

$$C = \frac{\partial^2 h}{\partial x^2} + \frac{\partial^2 h}{\partial y^2}, \quad (5)$$

where $h(x, y, t) = e(x, y, t) + S_a(x, y)$ is the altitude of the fluid surface. Equation (4) becomes then

$$\begin{cases} \sigma_{xz} = \gamma \left(\frac{\partial^3 h}{\partial x^3} + \frac{\partial^3 h}{\partial y^2 \partial x} \right) (h - z), \\ \sigma_{yz} = \gamma \left(\frac{\partial^3 h}{\partial y^3} + \frac{\partial^3 h}{\partial x^2 \partial y} \right) (h - z). \end{cases} \quad (6)$$

Equation (6) has been derived without making any assumptions on the paint rheology. However, the deviator stress tensor can be expressed as a rheology-dependent function of the strain rate tensor. It is consequently possible to link the velocity vector \mathbf{u} to the derivatives of the film altitude h , and to calculate the local flow, given the film topography h , by integrating the velocity:

$$\mathbf{q}(x, y) = \int_{S_a}^h \mathbf{u}(x, y, z) dz. \quad (7)$$

2.2 Inverse problem of flow determination

We rely on measurements of the film topography that are obtained at regular time intervals during the levelling process. By solving an inverse problem, it is possible to access the local flow rates within the film, without any hypothesis on the fluid rheology. The local altitude variation is indeed related to the local evaporation and the local flow gradients by the mass conservation equation:

$$\frac{\partial h}{\partial t}(x, y, t) = -\nabla \cdot \mathbf{q}(x, y, t) - E(x, y, t), \quad (8)$$

where $E(x, y, t)$ denotes evaporation. The direct problem described by (8) yields the local altitude variation knowing the local flow rate. We are interested in the inverse problem, which is to determine the local flow knowing the local altitude variation. A major difficulty in the study of such inverse problems is that the solution is rarely unique. A mathematical problem is said to be well-posed if it admits a unique solution that depends continuously on the data. The mathematical problem we are interested in is ill-posed. Indeed, it is obvious that if \mathbf{q}_1 is a solution, any flow writing $\mathbf{q}_1 + \mathbf{q}_2$ where $\nabla \cdot \mathbf{q}_2(x, y, t) = 0$ will also be a solution. In the framework of the lubrication approximation, as the gradients along \mathbf{x} and \mathbf{y} , and

the velocity along \mathbf{z} can be neglected, we can nevertheless add the physical condition

$$\text{curl curl } \mathbf{q} = \mathbf{0}. \quad (9)$$

Under this assumption, we have the following relation

$$\Delta \mathbf{q}(x, y, t) = -\nabla \left(\frac{\partial h}{\partial t}(x, y, t) + E(x, y, t) \right). \quad (10)$$

Estimating the right-hand side of (10), it becomes possible to access the flow rate by solving the Poisson equation, which allows us, on the one hand, to validate a model of rheology by comparing the flow values to those calculated with the model and, on the other hand, to determine the local rheological parameters of the fluid.

3 Experimental measurements

The method presented in the previous section was used to study the rheology of thin films of a lacquer used in the automotive industry within the few minutes after its deposit. Most of the flow occurs indeed at room temperature during this short period of time that we refer to as flash time. Measurements of the layer topography are performed at regular time intervals (1 s) with a high resolution wavefront sensor developed by PhasicsTM (<http://www.phasicscorp.com/>). The wavefront sensor uses a technology based on a modified Hartmann test to measure wavefront distortions. By means of a 2D diffraction grating, a beam is replicated into four identical waves that are propagated along slightly different directions. The direction differences create interference patterns that are used to reconstruct the measured surface topography. The main advantage of this experimental device is that it is able to measure a large painted surface with a high dynamics and a satisfying accuracy (the measurement error is less than a few μm), which allows us to take snapshots in sufficiently quick succession. The adjustment of the wavefront sensor is also robust, so that it is not necessary to readjust the device during the painting process.

The wavefront sensor probes $18 \text{ mm} \times 18 \text{ mm}$ surfaces. The large-scale components of the measured surfaces will be referred to as the shape. A shape extraction is achieved by the device during the measurement to correct optical aberrations. The topography is projected on a basis of spherical harmonic polynomials of empirically chosen degree. Nevertheless, the shape extraction is not perfect and a slight error remains in the topography.

3.1 Surface evolution

Figure 1 shows the evolution of the topography of a lacquer layer deposited on a smooth substrate at the beginning of the flash time. We observe a very rapid levelling of the

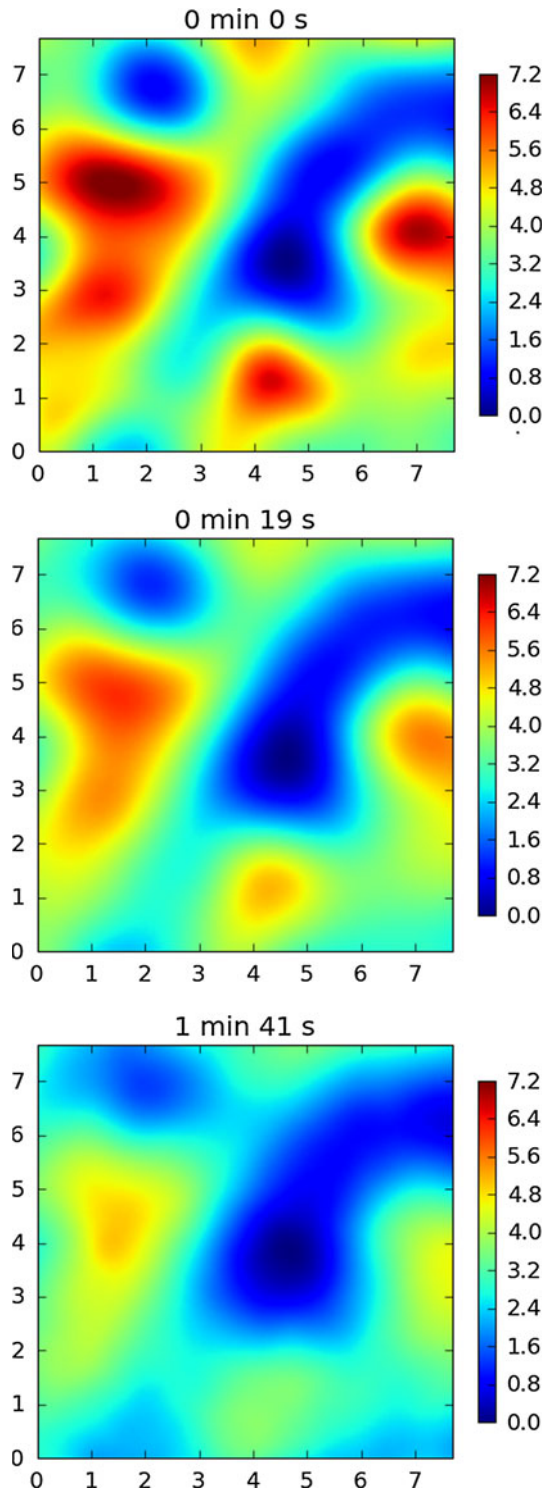


Fig. 1 Evolution of the lacquer layer topography measured with the wavefront sensor at the beginning of the flash time. The *horizontal scale* is given in mm and the *vertical scale* in μm . The precision of the vertical measurements is up to $1 \mu\text{m}$. On each surface, during measurements, the minimum is arbitrarily set to zero, as it is not possible to obtain absolute altitudes, but only relative ones with the device used

paint. This levelling is due to the combined effects of the rapid evaporation of light solvents and the flow caused by surface tension. The phenomenon is especially important at the beginning of the flash time when the viscosity of the painting is still relatively low. At the end of the flash time, the levelling slows down until the painted layer topography stops evolving.

3.2 Roughness characterization

The roughness of a surface corresponds to the elevation changes that distinguish this surface from a smooth one. As the physical effects that cause the film levelling occur at different scales, it is of interest to use tools to separate the roughness scales of the studied topographies. An algorithm based on the wavelet packet transform (Mallat 1999) and the reconstruction formula was developed that allows a decomposition of the roughness into the sum of its multiscale contributions (Zahouani et al. 2003; Figliuzzi et al. 2011).

Let f be a function in $L^2(\mathbb{R})$. As

$$\|f\|^2 = \int_{\mathbb{R}} f(x)^2 dx < \infty,$$

the function

$$x \rightarrow \frac{f(x)^2}{\|f\|^2}$$

can be viewed as a density of probabilities. We can then associate a mean spatial position to the function f ,

$$\bar{x} = \frac{1}{\|f\|^2} \int_{\mathbb{R}} xf(x)^2 dx,$$

and a variance around this mean position:

$$\sigma(f) = \frac{1}{\|f\|^2} \int_{\mathbb{R}} (x - \bar{x})^2 f(x)^2 dx.$$

Using the Plancherel theorem, we can also associate a mean position to the Fourier transform of f in the Fourier space,

$$\bar{\omega} = \frac{1}{2\pi\|\hat{f}\|^2} \int_{\mathbb{R}} \omega \hat{f}(\omega)^2 d\omega,$$

and a variance around this position:

$$\sigma(\hat{f}) = \frac{1}{2\pi\|\hat{f}\|^2} \int_{\mathbb{R}} (\omega - \bar{\omega})^2 \hat{f}(\omega)^2 d\omega.$$

A wavelet is a function ψ in $L^2(\mathbb{R})$ with zero average, normalized $\|\psi\| = 1$ and centred in the neighbourhood of

$t = 0$, which is well localized in both physical and Fourier space. We obtain a wavelet family $\{\psi_{u,s}, u \in \mathbb{R}, s > 0\}$ by dilating this function by a scale parameter $s > 0$ and translating it by $u \in \mathbb{R}$:

$$\psi_{u,s}(x) = \frac{1}{\sqrt{s}} \psi\left(\frac{x-u}{s}\right)$$

Let f be a function in $L^2(\mathbb{R})$. The wavelet transform of f is

$$Wf(u, s) = \int_{-\infty}^{+\infty} f(x) \frac{1}{\sqrt{x}} \psi\left(\frac{x-u}{s}\right) dx.$$

A wavelet coefficient corresponds to the projection of the function f on the wavelet $\psi_{u,s}$. A high value of a wavelet coefficient then indicates that the function f contains information at the scale s and at location u . It is possible to reconstruct the original function f using the wavelet coefficients:

$$f(x) = \frac{1}{C_\psi} \int_0^{+\infty} \int_{-\infty}^{+\infty} Wf(u, s) \frac{1}{\sqrt{x}} \psi\left(\frac{x-u}{s}\right) \frac{ds}{s^2} du.$$

In our case, the projection of the surface on a family of wavelets consequently allows to locally identify the scales of the surface corrugations. It is straightforward to generalize the wavelet transform formula and the reconstruction formula for two or more dimensions. Algorithms that are suitable to the case of numerical signals have been developed, for example, the orthonormal wavelet transform or the packet transform (Mallat 1999).

The idea behind the roughness characterization algorithm presented here is to decompose the studied surface S on a family of wavelet packets and to reconstruct it, keeping only the wavelet coefficients that correspond to each successive scale. The surfaces are sampled with an horizontal step $\Delta l = 60 \mu\text{m}$, which results in a 128 by 128 pixels image $S = S[n_1, n_2]$. The surface S is then decomposed in its multiscale components:

$$S[n_1, n_2] = \sum_{j=0}^J S_j[n_1, n_2], \tag{11}$$

where J denotes the number of scales. The use of the packet wavelet transform requires us to adopt a dyadic discretization of the scale parameter, which leaves us with seven octaves as we have 128 by 128 pixels image ($128 = 2^7$). We then introduce three intermediate scales in each octave $[2^j, 2^{j+1}]$ to improve the accuracy of the scale discretization. Finally, we are left with $J = 28$. $\forall j < J$, we have

$$S_j[n_1, n_2] = \sum_{k_1, k_2} Wf(k_{1,2}, 2^j) \frac{1}{\sqrt{2^j}} \psi\left(\frac{k_{1,2} - n_{1,2}}{2^j}\right).$$

For each reconstructed surface, it is possible to define a parameter, denoted Mq , that characterizes the mean deviation from the average surface at the scale j . The resulting Mq curve characterizes the frequential content of the roughness:

$$Mq[j] = \frac{1}{N^2} \sqrt{\sum_{n_1=1}^N \sum_{n_2=1}^N \left(\frac{S_j[n_1, n_2] - \bar{S}_j}{\Delta l}\right)^2}, \tag{12}$$

where \bar{S}_j denotes the mean value of S_j . The parameter Mq describe the contribution of each scale of the surface to the global roughness and allows us to observe scale by scale the influence of the physical effects that occur during the levelling of the paint.

4 Results and discussions

4.1 Estimation of the evaporation law

Using the surface characterization algorithms that have previously been presented, it is possible to separate, scale by scale, the physical effects that occur during the film levelling. Accordingly, we shall assume that the pattern attenuation at the largest scales is mainly caused by evaporation, since a levelling caused by surface tension would suppose a huge mass transport which would be unrealistic considering the geometric characteristics of the painted film. The surfaces measured with the wavefront sensor can be decomposed in their multi-scale components. At a specified time t , we have:

$$h(x, y, t) = \sum_{j=0}^J h_j(x, y, t), \tag{13}$$

where h denotes the film altitude, J the number of decomposition scales, and h_j the surface reconstruction from its projection on the wavelets of scale j . Assuming that the large-scale patterns attenuation is mainly caused by evaporation, if α denotes the evaporation rate for the large scale components, the evolution of the reconstructed surface is given by

$$h_j(x, y, t + \Delta t) = \alpha h_j(x, y, t). \tag{14}$$

By studying the evolution of the Mq parameter corresponding to the largest scales between two successive surfaces, it is consequently possible to estimate the evaporation rate experimentally.

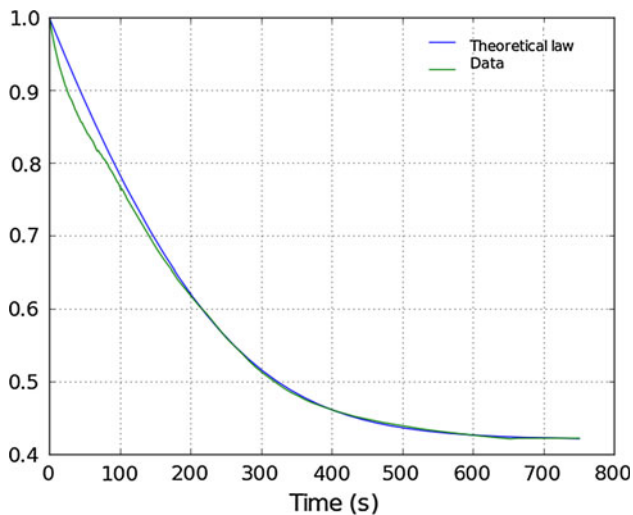


Fig. 2 Evaporation curve of the thin film of lacquer during the flash time: the experimentally measured curve deduced from the Mq parameter evolution is represented in *green*. The fitting curve is represented in *blue*

The chemical composition of the lacquer is complex, and many solvents are involved to avoid fast evaporation and to prevent immediate levelling of the film. Nevertheless, from a macroscopical point of view, evaporation can be modelled by a relatively simple law. To determine it, we assume that the paint is made of a resin in concentration $1 - c$ and a solvent in concentration c . We will assume evaporation E to be proportional to the solvent concentration:

$$E = \lambda c. \tag{15}$$

Denoting the film thickness by e and the final film thickness by e_∞ , the solvent concentration within the film is given by

$$c = \frac{e - e_\infty}{e}. \tag{16}$$

Neglecting the levelling caused by the surface tension, mass conservation reads

$$\frac{de}{dt} = -E. \tag{17}$$

Consequently,

$$\frac{de}{dt} = -\lambda \left(\frac{e - e_\infty}{e} \right). \tag{18}$$

The thickness evolution, assumed to correspond to the Mq parameter attenuation at the largest scales, is represented in green in Fig. 2. The film thickness is normalized to the unity. The theoretical evaporation law obtained from (18) is plotted in blue on the same figure. Parameter λ is estimated from experimental data by adjusting the theoretical and the experimental curves. Its value is given in Table 1.

Table 1 Simulation parameters

Parameter	Value	Value in Overdiep (1986)	Unit
γ_r	–	3.0×10^{-2}	N/m
γ_s	–	2.5×10^{-2}	N/m
η_0	–	1.0	Pa s
c_0	0.58	0.5	–
a	19	15 (Weidner et al. 1996)	–
λ	4.0×10^{-9}	2.0×10^{-9}	m/s
$\gamma_0/3\eta_0$	1.0×10^4	1.0×10^4	$\mu\text{m/s}$

The main difference between the two curves is observed at the beginning of the levelling. Many different solvents evaporate then, which increases the dynamics of the evaporation.

4.2 Resolution of the inverse problem

Given two successive film topographies, the inverse problem consists in determining the local flow rate. We saw earlier that the flow is a solution to Poisson equation

$$\Delta \mathbf{q}(x, y) = -\nabla \left(\frac{\partial h}{\partial t}(x, y) + E(x, y) \right). \tag{19}$$

Using the characterization algorithm described in the previous section, it was possible to estimate the evaporation term $E(x, y)$ and consequently the right-hand side of (19). When measuring the topographies using the wavefront sensor, an error on the shape of the measured surface is likely to remain due to optical aberrations during the process. To correct this error, a shape extraction is performed by projecting the right-hand side of (19) on a wavelet basis and by reconstructing it cancelling the highest scales components. To manage boundary effects, the surface is unfolded by mirror symmetry to remove the jumps at the interfaces. Assuming that the boundary conditions are periodic, we solve (19) using a spectral method. In Fourier space, denoting by f_x the component of the right-hand side along the \mathbf{x} axis, and by f_y its component along the \mathbf{y} axis, the equation reads:

$$\hat{f}_{x,y}(\xi_x, \xi_y) = -(\xi_x^2 + \xi_y^2) \hat{q}_{x,y}(\xi_x, \xi_y). \tag{20}$$

The flows expressions can easily be calculated in the Fourier space:

$$\hat{q}_{x,y}(\xi_x, \xi_y) = \frac{\hat{f}_{x,y}(\xi_x, \xi_y)}{\xi_x^2 + \xi_y^2}. \tag{21}$$

The local values of the flow rate can be derived from the previous equations by an inverse Fourier transform. It is important to notice that $\hat{f}_{x,y}(0, 0) = 0$. Indeed, denoting L the unfolded surface size,

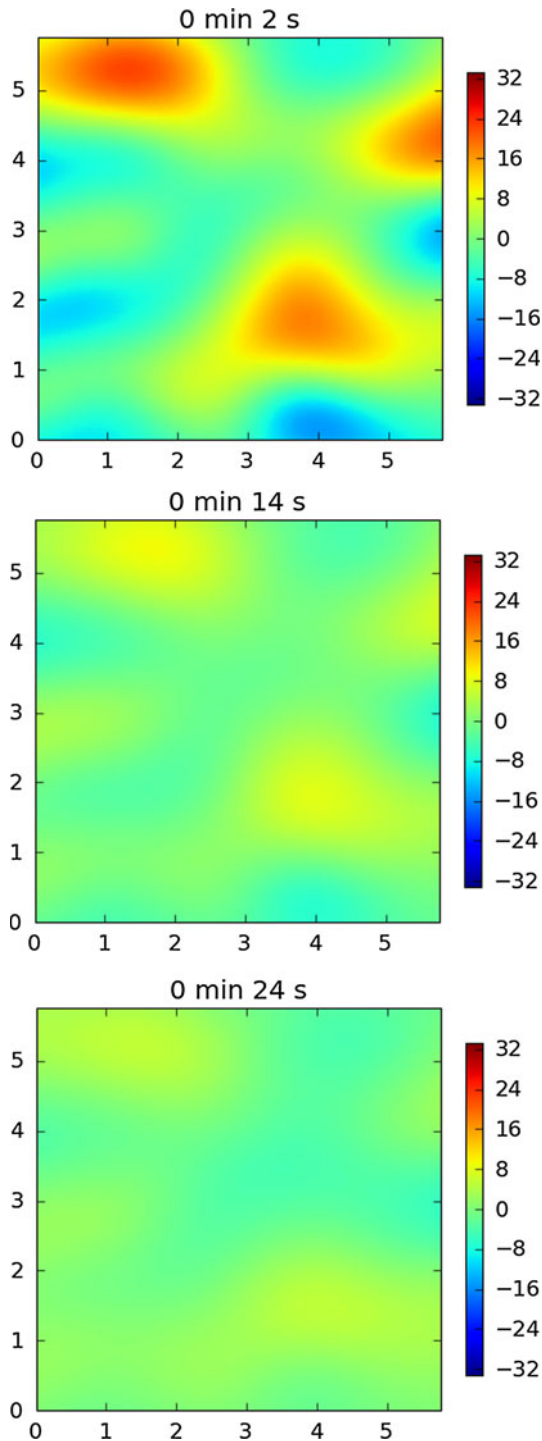


Fig. 3 X-component of the lacquer flow rate at the beginning of the flash time, obtained by solving the inverse problem. The flow map is represented in a *square image* of 128×128 pixels. Each *pixel value* represents the value of the mean flow averaged over $60 \mu\text{m} \times 60 \mu\text{m}$ surface. The *horizontal scale* is given in mm and the *vertical scale* in $\mu\text{m}^2/\text{s}$

$$\hat{f}_{x,y}(0,0) = \int_0^L \int_0^L f_{x,y}(x,y) dx dy. \quad (22)$$

This quantity cancels, as $\hat{f}_{x,y}(0,0)$ corresponds to the integral over a period of a continuous periodic function gradient.

Figure 3 shows the mapping of the flow-rate field obtained by solving the considered inverse problem at different moments of the flash time.

4.3 Newtonian model

Assuming a Newtonian rheology, the deviator stress tensor can easily be expressed as a function of the strain rate tensor:

$$\bar{\sigma} = \frac{\eta}{2} (\nabla \mathbf{u} + {}^T \nabla \mathbf{u}) \quad (23)$$

Consequently, the local flow components on the film thickness along the horizontal directions read

$$\begin{cases} q_x = \frac{\gamma}{3\eta} (h - S_a)^3 \left(\frac{\partial^3 h}{\partial x^3} + \frac{\partial^3 h}{\partial x \partial y^2} \right), \\ q_y = \frac{\gamma}{3\eta} (h - S_a)^3 \left(\frac{\partial^3 h}{\partial y^3} + \frac{\partial^3 h}{\partial y \partial x^2} \right). \end{cases} \quad (24)$$

As shown in Sect. 2, the formula allows the calculation of the flow from the topography of the thin film.

The expressions for the flow rate resulting from the Newtonian model are given by (24). These equations involve high-order spatial gradients of the film surface. If one wishes to calculate the flow by applying directly this model on the surfaces obtained with the wavefront sensor, we need efficient differentiation methods. The calculation of the spatial derivative of an experimental surface is far from trivial. The surfaces obtained through the wavefront sensor are indeed slightly noisy after the measurement, and the gradient operator is very sensitive to noise. In order to regularize the data, the spatial derivatives will consequently be calculated using Gaussian filtering. The gradient is calculated by convoluting the original surface with the kernel of the derivative of a centred Gaussian function of specified variance σ^2 :

$$G(x,y) = \frac{1}{2\pi\sigma} \exp\left(-\frac{x^2 + y^2}{2\sigma^2}\right). \quad (25)$$

We easily verify that

$$S * \frac{\partial G}{\partial x}(x,y) = G * \frac{\partial S}{\partial x}(x,y). \quad (26)$$

The result corresponds to the convolution product of the surface derivative with a Gaussian with variance σ^2 . The choice of the variance of the Gaussian kernel is fundamental, since it remains important to avoid losing too much physical information. Here, we empirically take $\sigma = 92 \mu\text{m}$: this value is on the same order of magnitude than the spatial step and allows to properly perform the

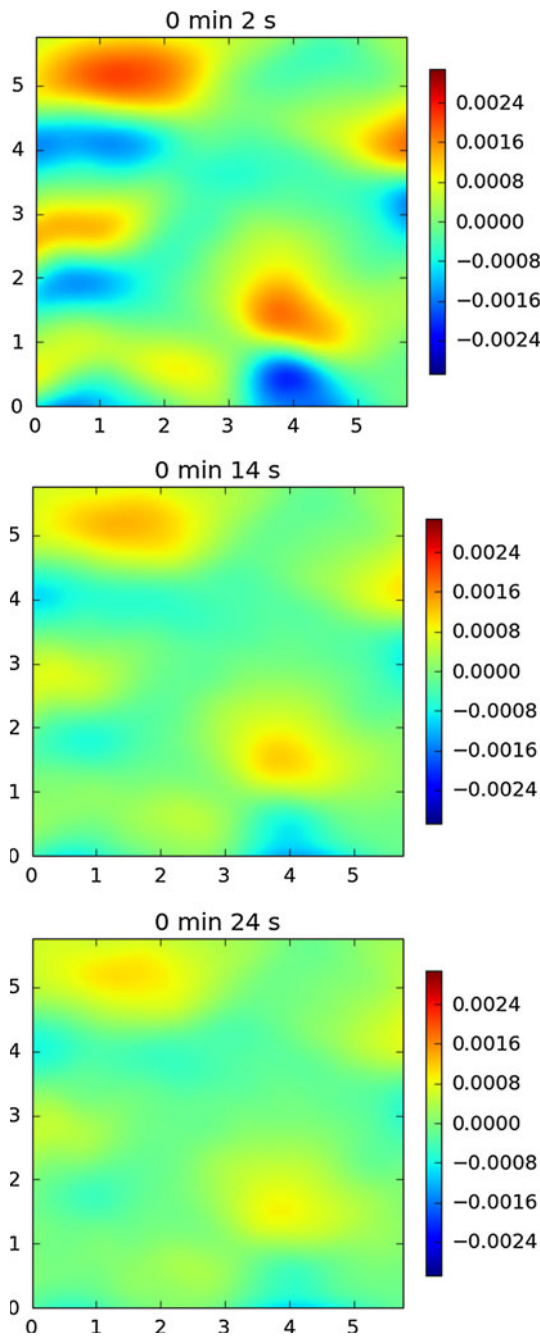


Fig. 4 Evolution of the quantity $\Psi = (h - S_a)^3(\partial_{xxx}h + \partial_{yyy}h)$ at the beginning of the flash time. The *map* is represented in a *square image* of 128 pixels by 128 pixels. Each *pixel value* corresponds to the mean value of $\Psi(x, y)$ on a $60 \mu\text{m} \times 60 \mu\text{m}$ surface. The *horizontal scale* is given in mm, and the *vertical scale* is given in μm

gradient calculations. Figure 4 shows the results of the flow direct simulation using the Newtonian model.

Power law models are often used to describe the rheology of paints such as electrophoresis. In our case, we find a good agreement between the Newtonian model and the experimental data and show that a Newtonian rheology explains the dynamics of the levelling for the considered

lacquer. It is not possible to improve the correlation coefficients by employing a power law model. A result of the measurement led during our study is then that a Newtonian model seems well-adapted to describe the rheology of the lacquer at the considered scales.

4.4 In situ estimation of the rheological parameters of the paint

By comparing the values of $\Psi = (h - S_a)^3(\partial_{xxx}h + \partial_{yyy}h)$ and the local flow calculated by solving the inverse problem point by point, we obtain the cloud of points of Fig. 5. If the fluid rheology is Newtonian, there exists a linear relation between both quantities, the proportionality coefficient being $\gamma/3\eta$. The results presented in the Fig. 5 show that the data are relatively well interpolated by a straight line during the flash time, which suggests that the fluid exhibits a Newtonian rheology. Figure 6 shows the evolution of the proportionality coefficient $\gamma/3\eta$. The following law is often proposed in the literature to link the surface tension to the solvent concentration:

$$\gamma = \gamma_r + c(\gamma_s - \gamma_r) = \gamma_r + c\Delta\gamma, \tag{27}$$

where γ_r denotes the surface tension of the resin, and γ_s the surface tension of the solvent. On the other hand, the viscosity depends on the solvent concentration through the exponential law

$$\eta(c) = \eta_0 e^{-ac}. \tag{28}$$

Using these laws to fit the experimental data, we find

$$\frac{\gamma}{3\eta}(c) = \frac{\gamma_r + c\Delta\gamma}{3\eta_0} e^{a(c-c_0)} \tag{29}$$

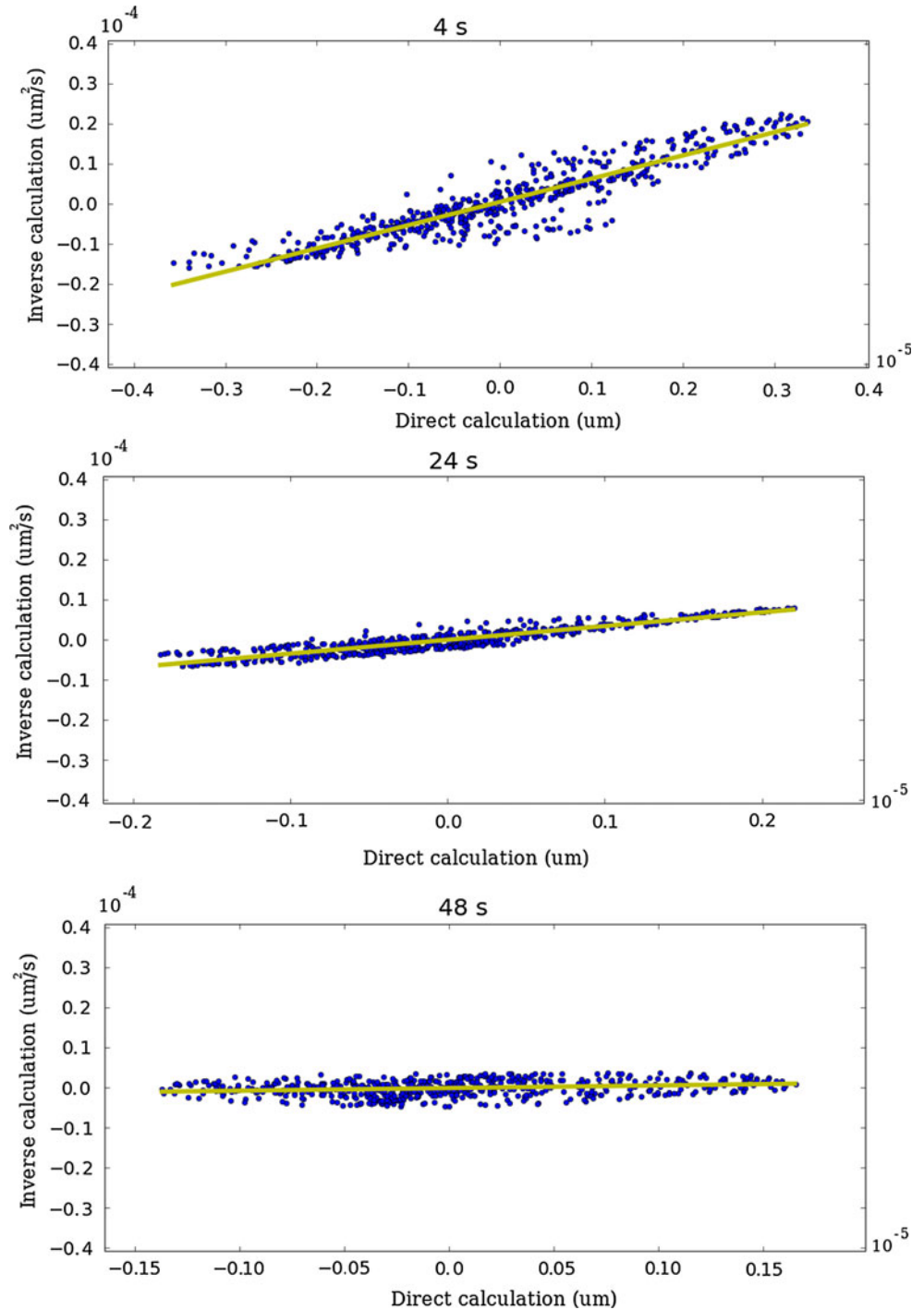
with $\gamma_0/3\eta_0 = 10,000 \mu\text{m/s}$, $c_0 = 0.58$ and $a = 19.0$, yielding rheological parameters very close to those measured by Overdiep (1986).

The parameters determined by solving the inverse problem were used to carry out numerical simulations of the evolution of the film topography for a Newtonian fluid, results of which are presented in Figliuzzi et al. (2012). The simulation results are very close to the experimental data, which shows that it is possible to accurately reproduce the levelling dynamics with the rheological parameters found in Table 1.

4.5 Discussion

Used in the case of a lacquer for the automotive industry, the characterization method presented in this paper allows the determination of physical parameters that correspond to the usual data found in the literature. An interesting result is, in particular, that the dynamic range of the wavefront sensor is high enough to make it possible to

Fig. 5 Flow rates calculated by the inverse method as a function of $\Psi = (h - S_a)^3 (\partial_{xxx}h + \partial_{xyy}h)$. The linear correlation coefficient ranges from 0.85 to 0.67



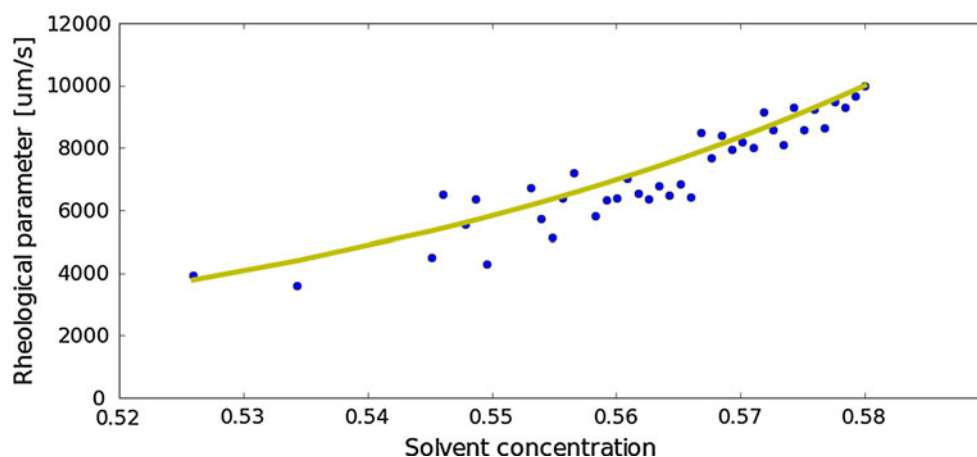
obtain a good estimate of the time derivative of the paint layer topography.

In practice, the method remains very sensitive to the influence of measurement noise and signal processing tools have to be developed to filter and exploit the experimental data. The main practical difficulty is the estimation of the evaporation coefficient. In our case, this estimation is performed using the wavelet transform algorithm described in this paper. This approach proves very useful to separate

the physical effects at different scales and to isolate the patterns whose levelling is uniquely led by evaporation.

Other difficulties arise from the measurements errors: due to optical aberrations, a shape error remains on the topographies. The wavelet transform is used to isolate the largest scales of the surfaces, and a correction is applied on these scales. However, it is very difficult to correct the shape, and a small error remains, that impacts both the estimation of the evaporation coefficient, done on the

Fig. 6 Experimentally determined values of the rheological parameter $\gamma/3\eta$, compared with predictions of the corresponding theoretical law (29) using coefficients reported in Table 1



largest scales of the surface, and the results of the inverse problem.

The high-frequency measurement noise also deeply affects the results. If the linear correlation coefficient is close to one at the beginning of the flash time, the data are extremely noisy later in the process of painting, and the correlation coefficient decreases. Indeed, the physical effects of the surface tension tend to become very slow as the viscosity increases within the paint film and, as the film evaporates and loses solvent, it tends to diffuse light more, which affects the quality of the data collected with the wavefront sensor. It becomes then difficult to separate the physical effects from the noise. The method therefore cannot be applied to the long-time evolution of the lacquer. However, in the present case, most of the levelling occurs during the flash time. At long times, as very low flow rate prevails, behaviours such as thixotropy could be reasonably expected.

Finally, as the direct calculation of the flow involves high-order gradients of the surface probed by the wavefront sensor, it is necessary to slightly filter the data in order to appropriately calculate the surface spatial gradients. Due to Gaussian filtering performed on the data, the results obtained by solving the inverse problem and consequently the modelling of flow phenomena are valid only for scales ranging from 100 μm to 1 cm. Small particles, with sizes close to 1–10 μm , are involved in the composition of the lacquer. The presence of these particles is likely to change the lacquer rheology fundamentally at smallest scales, where a non-Newtonian rheology should be observed.

5 Conclusion

In this paper, we have presented a method to characterize the rheology of a thin film from measurements at regular time intervals of its surface topography. By solving an inverse problem, we showed that it was possible to validate a model of rheology for the film and to estimate its

rheology parameters. In practice, some difficulties arise due to measurement noise. Specific methods based on the wavelet transform have been used to properly exploit the experimental data. The method was applied to the study of a lacquer used in the automotive industry. Despite some weakness due to the sensitivity to measurement noise, the method validates the assumption that the paint exhibits a Newtonian behavior at scales ranging from 100 μm to 1 cm, and estimates parameters that are close to those found in the literature for a fluid with similar properties. The measurements obtained with the wavefront analyser open interesting prospects for studying the fluids rheology in the thin films geometric configuration. These observations combined with numerical simulations of the evolution equations of the fluid elevations on a rough surface open the way to in situ rheological measurements of thin films. In the case of the painting process, such measurements could help the paint makers to better understand the physical properties of their paintings and to improve their properties. An accurate knowledge of the physical phenomena involved during the painting process could finally help steel makers to optimize the roughness of their sheets.

Acknowledgments This work has been supported by ArcelorMittal Research. The authors are grateful to anonymous referees, who helped to improve the initial version of the paper.

References

- Eres MH, Weidner DE, Schwartz LW (1999) Three-dimensional direct numerical simulation of surface-tension-gradient effects on the leveling of an evaporating multicomponent fluid. *Langmuir* 15:1859–1871
- Evans PL, Schwartz LW, Roy RV (2000) A mathematical model for crater defect formation in a drying paint layer. *J Colloid Interface Sci* 227:191–205
- Figliuzzi B, Jeulin D, Fricout G, Piezanowski JJ (2011) Surfaces characterization by means of wavelet analysis. In: 13th

- international conference on metrology and properties of engineering surfaces
- Figliuzzi B, Jeulin D, Lemaitre A, Fricout G, Piezanowski JJ, Manneville P (2012) Numerical simulation of thin paint film flow. *J Math Indust* 2
- Gaskell PH, Jimack PK, Sellier M, Thompson HM, Wilson MCT (2004) Gravity-driven flow of continuous thin liquid films on non-porous substrates with topography. *J Fluid Mech* 509:253–280
- Gaskell PH, Jimack PK, Sellier M, Thompson HM (2006) Flow of evaporating gravity-driven thin liquid films over topography. *Physics of fluid* 18:013601
- Howison SD, Moriarty JA, Ockendon JR, Terrill EL (1997) A mathematical model for drying paint layers. *J Eng Math* 32:377–394. doi:[10.1023/A:1004224014291](https://doi.org/10.1023/A:1004224014291)
- Mallat S (1999) A wavelet tour of signal processing, 2nd edn. Academic Press, New York
- O'Brien SBG, Schwartz LW (2002) Theory and modeling of thin film flows. In: Hubbard AT (ed) *Encyclopedia of surface and colloid science*. Santa Barbara Science Project, California, USA, 1st edn, CRC Press, pp 5283–5297
- Orchard SE (1961) On surface levelling in viscous liquids and gels. *Appl Sci Res* 11:451–464
- Oron A, Davis SH, Bankoff SG (1997) Long scale evolution of thin liquid films. *Rev Mod Phys* 69(3):931–980
- Overdiep WS (1986) The levelling of paints. *Prog Org Coat* 14:159–175
- Ruyer-Quil C, Manneville P (1998) Modeling film flows down inclined planes. *Eur Phys J B* 6:277–292
- Ruyer-Quil C, Manneville P (2000) Improved modeling of flows down inclined planes. *Eur Phys J B* 15:357–369
- Schwartz LW, Roy RV, Eley R, Petrash S (2001) Dewetting patterns in a drying liquid film. *J Colloid Interface Sci* 234:363–374
- Weidner DE, Schwartz LW, Eley RR (1996) Role of surface tension gradients in correcting coating defects in corners. *J Colloid Interface Sci* 179:66–75
- Wilson SK (1993) The levelling of paint films. *IMA J Appl Math* 50:149–166
- Zahouani H, Pokossi SE, Mezghani S, Vargiolu R, Jacobs H, Piezanowski JJ (2003) Characterization of the painted surfaces appearance by continuous wavelet transform. In: 9th international conference on metrology and properties of engineering surfaces